Journal of Structural Geology, Vol. 12, No. 4, pp. 453 to 469, 1990
Printed in Great Britain

0191-8141/90 $03.00+0.00

Structural evolution of the schist belt, south-central Brooks Range fold and thrust belt, Alaska

RICHARD R. GOTTSCHALK

Rice University, Department of Geology and Geophysics, Houston, TX 77251, U.S.A.

(*Received* 27 *February* 1989; *accepted in revised form* 3 *December* 1989)

Abstract—The schist belt is a *HP–LT* metamorphic belt derived from Lower Paleozoic and Proterozoic (?) continental protoliths, exposed in the hinterland of the Brooks Range fold and thrust belt, Alaska. Polyphase structures in the schist belt provide a record of deep-crustal processes during arc–continent collision and subsequent intracontinental contraction. The oldest structures are poorly preserved isoclines and sheath folds that formed under glaucophane-stable metamorphic conditions (D_{1a}); geometries of D_{1a} structures are consistent with formation during S-directed subduction of continental crust beneath the Yukon–Koyukuk island-arc (Late Jurassic–Early Cretaceous). D_{1b} and D_{1c} structures formed within thrust sheets of previously subducted material as *HP–LT* metamorphics were uplifted along S-dipping thrust faults (Early Cretaceous); minor N–S extension in the schist belt (recorded by ductile shear bands) probably occurred at shallow structural levels within the uplifting metamorphic welt (late Early Cretaceous). South-vergent D_2 folds may be related to N-directed underthrusting of the Yukon–Koyukuk arc beneath previously imbricated continental rocks, or to formation of the Doonerak Window duplex. D_3 folds resulted from E–W compression, possibly related to differential movement between the Siberian and Arctic Alaskan portions of the North American (Late Cretaceous ?).

INTRODUCTION

THE BROOKS RANGE fold and thrust belt (Fig. 1) comprises the external portion of a collisional orogen involving rocks exposed over much of northern and interior Alaska (Box 1985). Deformation is believed to result from the impingement of an island-arc on the Atlantic-style margin of the Arctic Alaskan continental microplate (cf. Hubbard *et al.* 1987) in the Late Jurassic or Early Cretaceous (Roeder & Mull 1978, Mull 1982, Mayfield *et al.* 1983, Patton 1984, Box 1985); remnants of the continental margin sequence are extensively exposed in the Brooks Range, and the island-arc assemblage crops out sporadically in the western and central Yukon–Koyukuk basin. Arc–continent collision presumably initiated with the subduction of oceanic crust beneath the Yukon–Koyukuk island-arc (Mayfield *et al.* 1983, Box 1985), resulting in closure of the intervening ocean basin or back-arc basin. Emplacement of the arc on the continental margin resulted in N-directed obduction of oceanic crustal fragments (Roeder & Mull 1978, Pallister & Budahn in press), and the imbrication of continental margin sediments (Mayfield *et al.* 1983). Compressional deformation in the Brooks Range continued through the Tertiary and possibly later time (Hubbard *et al.* 1987, Oldow *et al.* 1987a) with the emplacement of the accreted terranes that make up the southern Alaskan lithotectonic collage (Oldow *et al.* 1989a).

In its structural style, the Brooks Range is typical of thin-skinned, décollement-style fold and thrust belts. Deformation in the foreland is characterized by thrust faulting and folding of Upper Devonian to Mississippian clastic sediments (MDs, Fig. 1), Mississippian through Jurassic platformal clastics, carbonates and cherts (Ml), and Cretaceous foreland basin sediments (Kf). To the south, older, more highly deformed and metamorphosed rocks are exposed; these include the Cambrian through Silurian (Dutro *et al.* 1976, 1984, Moore & Churkin 1984) phyllites and metavolcanic rocks of the Doonerak Window (ЄSd), and the Cambrian through Devonian (Brosgé *et al.* 1979, Dillon *et al.* 1987, Boler 1989) metaclastic rocks and carbonates (ЄDs) of the Skajit allochthon (cf. Oldow *et al.* 1987a). Rocks representing the deepest structural levels exposed in the central Brooks Range crop out in a regionally extensive, E–W-trending belt of high-pressure–low-temperature (*HP–LT*) metamorphic rocks informally known as the schist belt (PzPm). The schist belt is derived in large part from epicontinental clastic, volcanic and carbonate protoliths (Hitzman *et al.* 1986), and is locally intruded by granitic rocks derived from a continental source region (Nelson *et al.* 1989).

There has been much confusion regarding the age and tectonic significance of *HP–LT* metamorphism in the southern Brooks Range due to difficulties in obtaining reliable metamorphic age dates. Turner *et al.* (1979) originally proposed that *HP–LT* metamorphism was Proterozoic in age, based on K–Ar ages on low-potassium metamorphic amphiboles. A recent isotopic age-dating survey by Armstrong *et al.* (1986), however, suggests that *HP–LT* regional metamorphism in the schist belt is more likely to be Late Jurassic to Early Cretaceous in age, a contention which is consistent with the existence of *HP–LT* assemblages in Middle Paleozoic metasedimentary rocks (Hitzman *et al.* 1986) and Devonian granitic plutons (B. E. Patrick personal communication 1989). Based on these age relations, it has been proposed that the Brooks Range schist belt and the correlative Seward Peninsula blueschists represent rem-

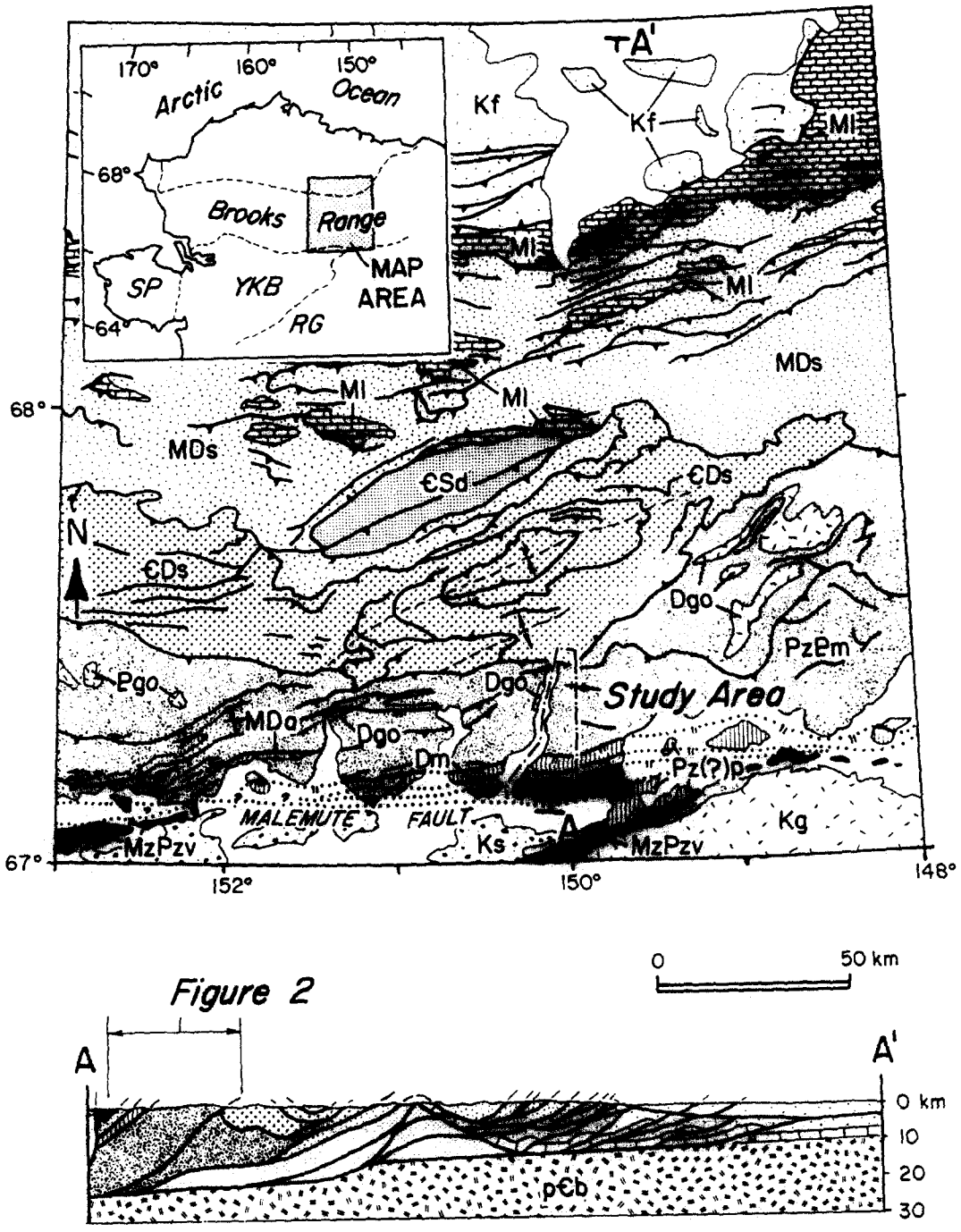

Fig. 1. Generalized geologic map of central Brooks Range with geologic cross-section, modified from Oldow *et al.* (1987a). Kf, Cretaceous foreland basin deposits. Ks, Lower Cretaceous sedimentary rocks of Koyukuk basin. Kg, Cretaceous granite. Ml, Mississippian Lisburne Limestone, Kayak Shale and Kekiktuk Conglomerate; Permian–Jurassic Sadlerochit Group, Shublik and Kingak Formations. MDs, Mississippian–Devonian Endicott Group clastic rocks, Devonian Beaucoup Formation. €Sd, Cambrian–Silurian metasedimentary and metavolcanic rocks of Doonerak window. €Ds, Cambrian–Middle Devonian rocks of Skajit allochthon. PzPm, Precambrian (?) and Paleozoic metamorphic rocks of schist belt. MDa, Mississippian–Devonian Ambler volcanogenic sequence. Dgo, Devonian granitic orthogneiss. Pgo, Precambrian (?) granitic orthogneiss. Dm, Devonian metagreywacke. Pz(?)p, undated phyllite. PzMzv, Paleozoic–Mesozoic basalt and chert of Angayucham terrane. p€b, Precambrian basement. SP, Seward Peninsula. YKB, Yukon–Koyukuk basin. RG, Ruby Geanticline. Thin lines, geologic contacts. Heavy lines: with barbs are thrust faults, teeth on upper plate; with hatchures are low-angle normal faults, hatchures on upper plate; without ornamentation are steeply dipping faults.

nants of a paleo-subduction zone of Late Jurassic–Early Cretaceous age (Forbes *et al.* 1984, Thurston 1985, Gottschalk 1987, Patrick 1988, Till 1988, Till *et al.* 1988). These authors suggest that the continental rocks of the schist belt and Seward Peninsula were subjected to *HP–LT* metamorphic conditions when partially subducted beneath the Yukon–Koyukuk island-arc, following the consumption of oceanic crust.

The study of polyphase structures in the schist belt provides an unique opportunity to characterize deep-crustal processes during arc–continent collision in northern Alaska. The purpose of this paper is to outline a

deformational and metamorphic history for the schist belt in the central Brooks Range based on the kinematic analysis of superposed folds, and on detailed microstructural and textural analysis. It will be shown that sequentially formed structures in the schist belt are consistent with formation during a single, protracted event of N–S-directed compression (in present day co-ordinates) related to collisional tectonism and subsequent intracontinental contraction. Structural relations in the schist belt provide constraints on: (1) the mechanics of continental subduction in central Alaska; (2) the mode of emplacement of previously subducted continental rocks into the Brooks Range fold and thrust belt; and (3) relationships between extensional deformation in the hinterland of the Brooks Range (Box 1987, Gottschalk 1987, Miller 1987, Oldow *et al.* 1987b, Gottschalk & Oldow 1988, Harris 1988, Avé Lallemant *et al.* 1989, Christiansen 1989), uplift of *HP–LT* metamorphic rocks, and contractional deformation.

GENERAL GEOLOGY OF THE STUDY AREA

The study area transects the schist belt immediately east of the Trans-Alaska pipeline in the south-central Brooks Range (Fig. 1). Here, the metamorphic rocks of the schist belt are exposed in a broad, asymmetric antiform, informally referred to herein as the Wiseman arch (Fig. 2). The 7 km structural section of continuously exposed metamorphic rock is essentially unbroken except for a few high-angle (?) faults with minor vertical displacement. To the east and west of the study area, the schist belt is dismembered by a number of widely-spaced, S-dipping thrust faults (Brosgé & Reiser 1964, 1971, Dillon *et al.* 1986).

The schist belt in the study area and vicinity is made up chiefly of undated pelitic and semi-pelitic quartz–mica schists, with subsidiary lenticular horizons of mafic schist, metagabbro, albite-schist, calc-schist, marble, granitic orthogneiss, metachert and eclogite. Pelitic and semi-pelitic schists are interlayered on a scale of centimeters to meters, and are probably derived from interbedded organic-rich shales and siliciclastic sediments. Marble and calc-schist lenses, along with scattered occurrences of calcite-bearing metapelites, indicate that the protolith was locally limy, and along with sparse metachert horizons, suggest a marine derivation for the sedimentary protolith. The metasedimentary sequence is locally intruded by Devonian granitic rocks (Dillon *et al.* 1980, 1986) and may correlate with western Brooks Range exposures of the pre-Devonian (?) Kogoluktuk schist or the lower portion of the Devonian (?) Anirak schist (of Hitzman *et al.* 1986).

Metamorphic rocks in the study area and vicinity are made up mainly of greenschist facies mineral assemblages (chlorite + albite + epidote + actinolite + sphene in metabasites, and quartz + phengite + paragonite + chlorite ± albite ± chloritoid in pelitic and semi-pelitic schists). There is, however, considerable evidence that the rocks were affected by a *HP–LT* metamorphic event which pre-dated recrystallization under greenschist facies conditions: (1) pseudomorphs after glaucophane are common, particularly in pelitic and semi-pelitic schists; (2) Till *et al.* (1988) report rare white mica + epidote pseudomorphs after lawsonite in metabasites; (3) eclogite occurs within the study area, and is

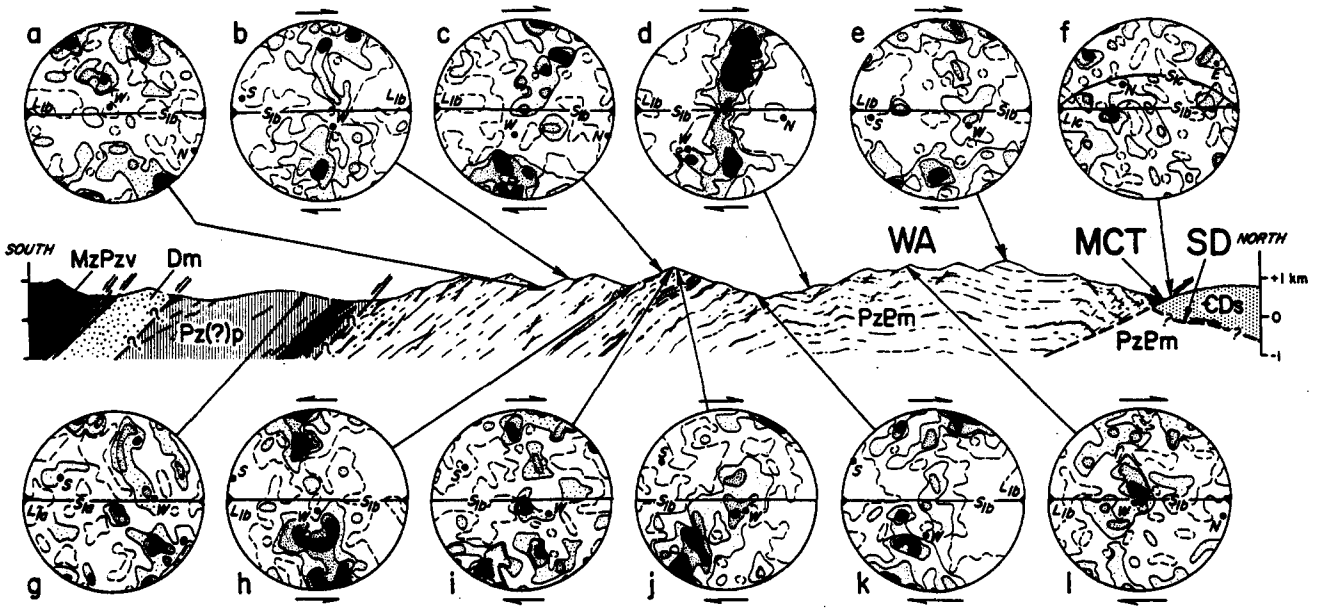

Fig. 2. Generalized geologic cross-section through study area. Geologic units same as Fig. 1. WA, Wiseman arch. MCT, Minnie Creek thrust. SD, Skajit décollement. Units in schist belt(PzPm): unornamented, pelitic and semi-pelitic schist; stipple, albite schist; black, metabasite; cross-hatch, calc-schist and marble. Ornamentation in schist belt: solid lines, S_{1b} form surfaces; post-S_{1b} extensional shear bands shown schematically, and not to scale. Units in phyllite belt (Pz(?)p): vertical rule, metapelite; black, metabasite. Also shown are lower-hemisphere, equal-area projections of quartz *c*-axes from oriented samples, $n = 200$ each sample. Sample locations projected onto geologic cross-section. Contours are 0.5, 1.5, 2.5 and 3.5% per 1% area. Solid line, foliation. Filled diamond, lineation. Filled circles, geographic co-ordinates. Arrows indicate sense of shear.

partially overprinted by greenschist facies assemblages (Gottschalk 1987); (4) Patrick (personal communication 1989) reports *HP–LT* metamorphic assemblages in granitic orthogneisses which intrude along-strike equivalents of rocks exposed in the study area; (5) crossite + epidote-bearing metagabbro crops out along the pipeline, near the southern boundary of the schist belt.

Along its northern boundary and to the east of the study area, the schist belt is structurally overlain by the lower grade metasediments of the Skajit allochthon (Brosgé & Reiser 1964, Oldow *et al.* 1987a). In this paper, the structure which separates the Skajit allochthon from the underlying schist belt is informally referred to as the Skajit décollement. Oldow *et al.* (1987a) argue that the Skajit décollement is the roof thrust of a crustal-scale duplex structure, whose formation involved imbrication of the Lower Paleozoic and Precambrian (?) rocks of the schist belt and their basement.

To the west of the study area, the schist belt structurally overlies the Skajit allochthon along the Minnie Creek thrust (Oldow *et al.* 1987a, Gottschalk & Oldow 1988) (Fig. 2). Regional mapping by Brosgé & Reiser (1964, 1971) and Dillon *et al.* (1986) indicates that the Minnie Creek thrust is a shallowly S-dipping fault along which the schist belt has been thrust northward over the Skajit allochthon metasediments. Oldow *et al.* (1987a, 1989b) have argued that offset on the Minnie Creek thrust post-dated duplexing of the schist belt beneath the Skajit allochthon, and resulted from breaching of the duplex roof fault.

The schist belt is structurally overlain along its southern boundary by a series of allochthons composed of distinctly lower grade metasedimentary and igneous rocks. These are, from north to south and structurally lowest to highest: (1) the undated, pumpellyite–actinolite facies metamorphic rocks of the phyllite belt (Pz(?)p, Figs. 1 and 2); (2) the low-grade Devonian (Gottschalk 1987, Murphy & Patton 1988) metasedimentary rocks of the metagreywacke belt (Dm); and (3) the prehnite–pumpellyite facies, Devonian through Jurassic pillow basalts and radiolarian cherts of the Angayucham terrane (Jones *et al.* 1988) (MzPzv). Gottschalk & Oldow (1988) and Avé Lallemant *et al.* (1989) have argued that low-grade allochthons along the southern flank of the schist belt are separated from the *HP–LT* metamorphics by a series of S-dipping normal faults with down-to-the-south offset.

STRUCTURES IN THE SCHIST BELT

The chronological notation (D_1, L_1, D_2, L_2, etc.) traditionally utilized by geologists in multiply deformed metamorphic terrains implies that successive structures in deforming rock masses form homogeneously and simultaneously over large areas. A simple chronological approach to superposed folding in the schist belt is misleading, however, because the number of fold phases varies as a function of local cumulative strain. For this reason, the concept of transposition cycles (Tobisch & Paterson 1988) is adopted to describe polyphase structures in the schist belt. In this paper, the first transposition cycle produced during a single progressive deformational event is designated D_{1a}, the second cycle, D_{1b}, and so on. Folds are designated with a different numerical subscript (e.g. D_2) when it can be demonstrated that they formed within a differing stress field or strain regime than their predecessors.

D_{1a}

The oldest structures in the schist belt (D_{1a}) are isoclinal folds and sheath folds with wavelengths ranging from a few mm to about 10 cm (Fig. 3a). These structures are present throughout the metamorphic pile, but are poorly preserved due to extensive deformation and recrystallization associated with later fold phases. Although it was not possible to directly measure the orientations of D_{1a} fold axes, type-3 interference patterns (Ramsay 1967) are produced where D_{1a} folds are refolded by later D_{1b} folds (Fig. 4), indicating that the axes of D_{1a} isoclines and sheath folds trend N–S, parallel to D_{1b} fold axes.

D_{1a} folds are associated with a penetrative axial-planar foliation (S_{1a}) that generally parallels lithologic layering. In pelitic and semi-pelitic schists, S_{1a} is defined by the differentiated layering of quartz with micas and (or) chlorite; in more massive rock-types, such as mafic schist, albite schist, and marble, S_{1a} is commonly indistinguishable from post-D_{1a} metamorphic fabrics. Poles to S_{1a} form an E–W-trending girdle due to isoclinal folding of S_{1a} about N–S-trending, subhorizontal D_{1b} fold axes (Fig. 5a).

Metamorphic textural criteria (Zwart 1962, Spry 1969) indicate that D_{1a} deformation took place under glaucophane-stable (*HP–LT*) metamorphic conditions. Idiomorphic pseudomorphs of albite + chlorite ± quartz after glaucophane are intergrown with phengite, paragonite, quartz, chlorite and chloritoid, all of which comprise S_{1a} in pelitic and semi-pelitic schists. Although relicts of *HP–LT* metamorphic minerals and mineral assemblages are also found in metagabbro and eclogite, they cannot be texturally related to D_{1a} since penetrative deformational fabrics are not developed in these rocks.

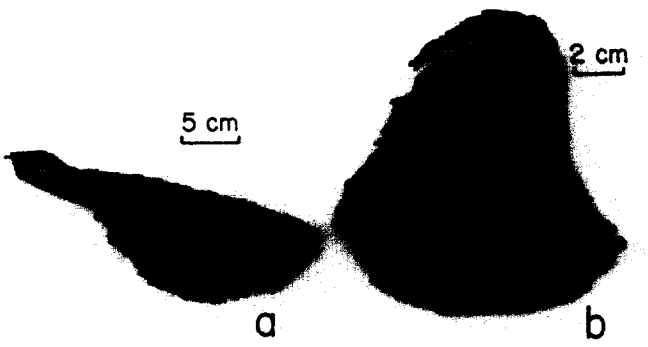

Fig. 4. Type-3 interference patterns produced by refolding of (a) a D_{1a} isoclinal fold and (b) a D_{1a} sheath fold.

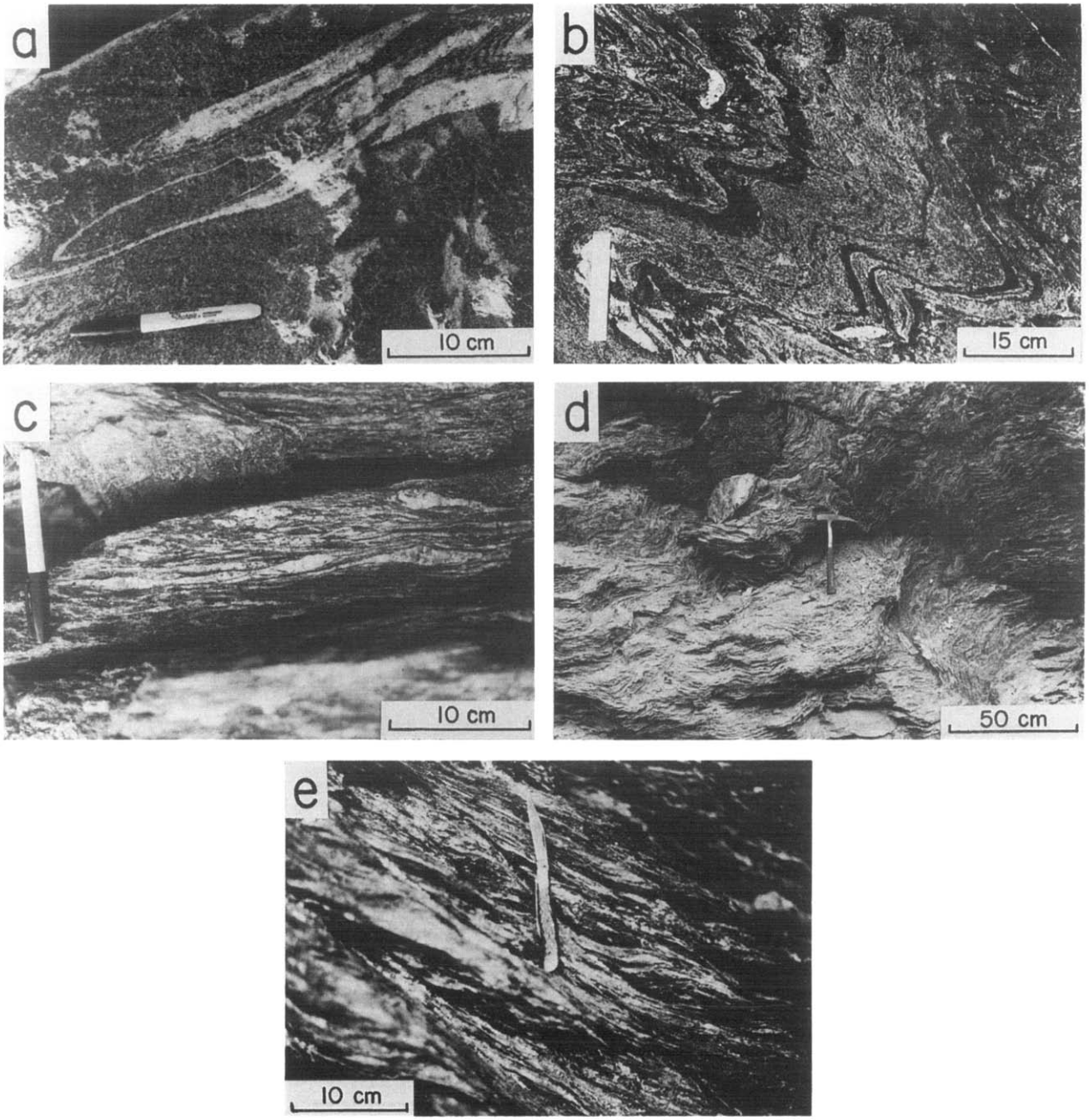

Fig. 3. Mesoscopic fold styles in schist belt. (a) D_{1a} sheath folds and isoclinal folds in semi-pelitic schist. (b) Close to tight D_{1b} folds in interlayered pelitic and semipelitic schist with penetrative axial-planar crenulation cleavage (S_{1b}). (c) Differentiated crenulation cleavage (S_{1b}) created by transposition of foliation (S_{1a}) in isoclinally folded pelitic schist. Where syn-D_{1a} quartz-segregations are involved in folding, rootless hinges and boudinaged limbs are present. (d) Asymmetric, N-vergent D_{1c} folds near Minnie Creek thrust. (e) Extensional shear band cleavage in pelitic schist. Folded surface is S_{1b}.

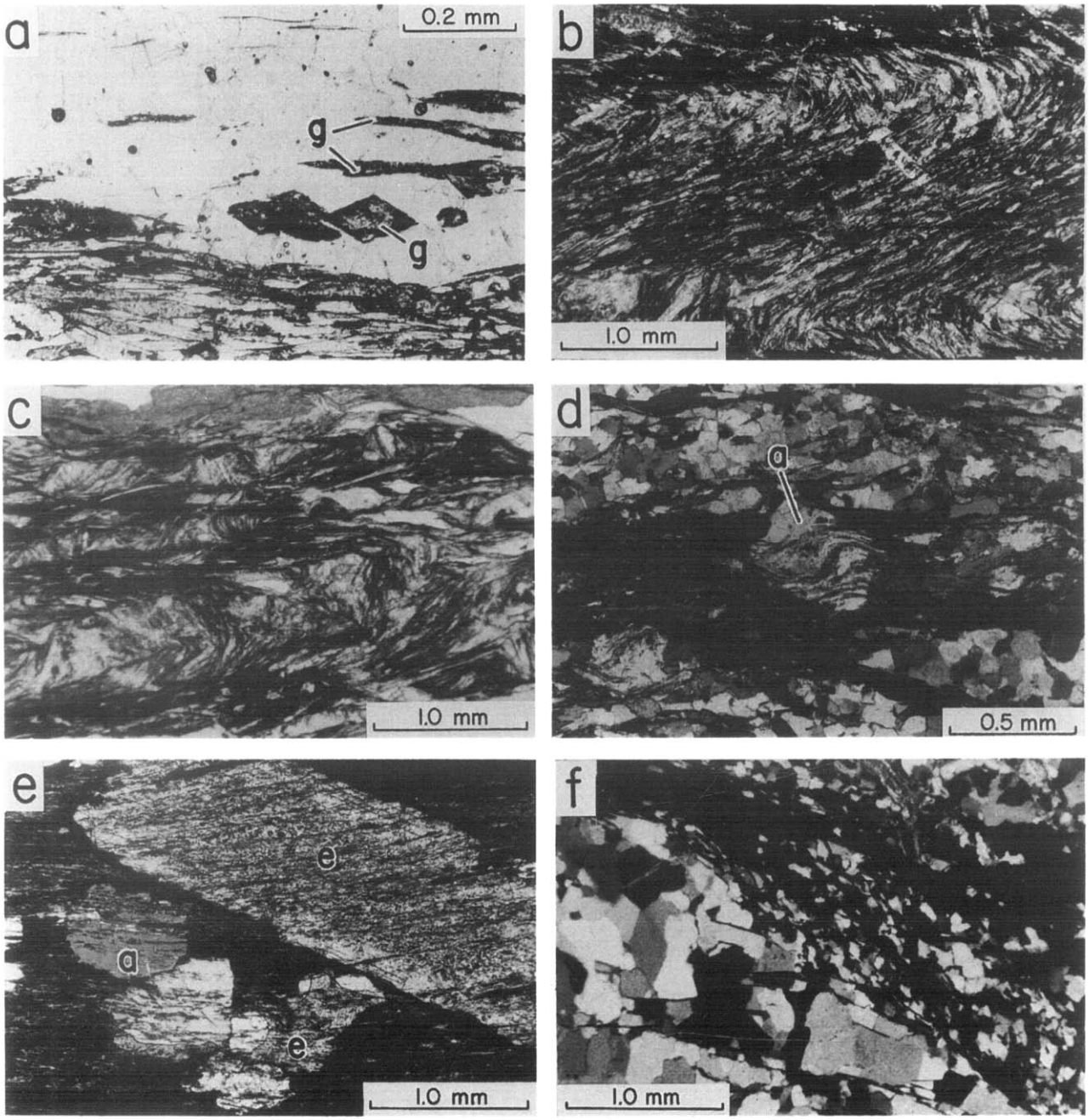

Fig. 6. Photomicrographs of microstructures and textures. (a) Pseudomorphs after syn-D_{1a} glaucophane (g) composed of randomly oriented intergrowth of albite + chlorite ± quartz, from pelitic schist. Other S_{1a} minerals in photomicrograph are white mica, chlorite and quartz. (b) Zonal crenulation cleavage (S_{1b}), showing D_{1b} fold hinges overprinted by post-D_{1b} white micas. (c) Discrete crenulation cleavage (S_{1b}) in isoclinally folded pelitic schist. (d) D_{1b} synkinematic albite porphyroblast (a) in pelitic schist. Graphitic inclusions in albite are continuous with S_{1b} in surrounding rock. (e) Idioblastic post-D_{1b} epidote (e) and albite (a) porphyroblasts in mafic schist. (f) Extensional shear band in pelitic schist, showing reduced grain size of dynamically recrystallized quartz. Shear zone also contains oriented neoblasts of chlorite and white mica.

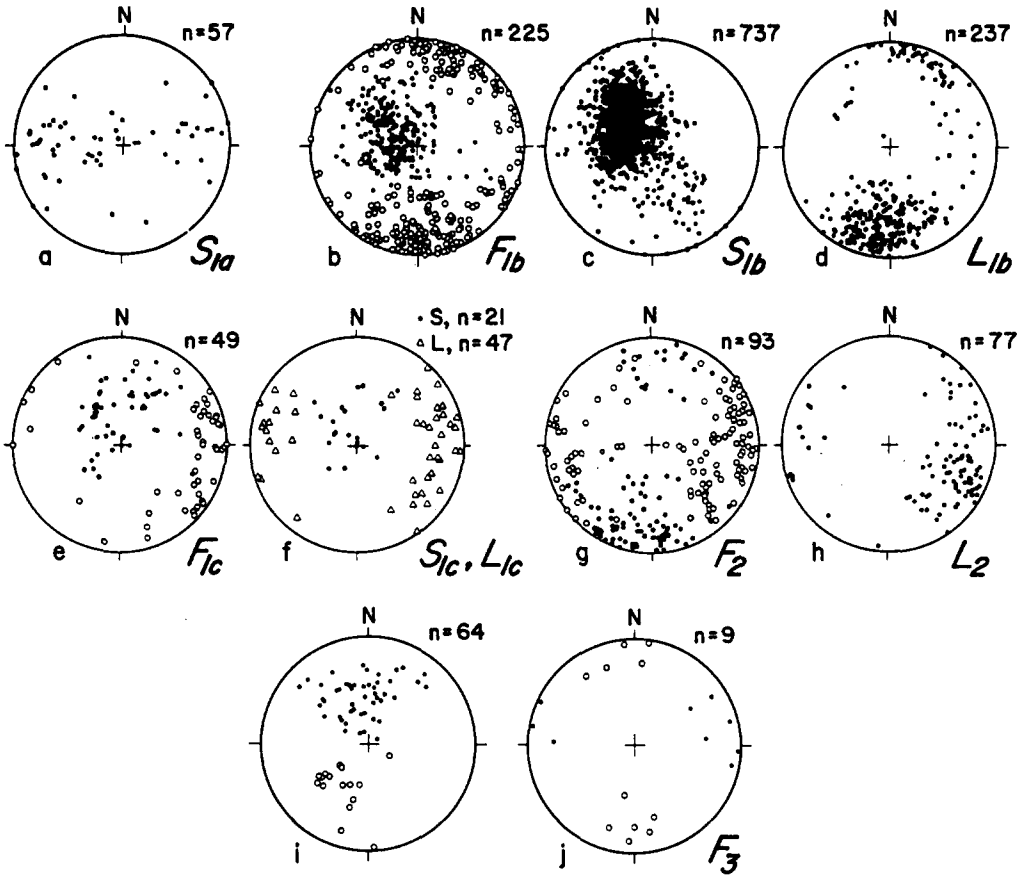

Fig. 5. Lower-hemisphere, equal-area stereographic projections of fold and fabric elements, F = folds, S = penetrative surfaces, L = lineations. For (b), (e), (g) and (j), filled circles = poles to axial planes; open circles = fold axes. For (i) filled circles = poles to extensional shear band cleavage with down-to-the-south offset, south flank of Wiseman arch; open circles = poles to extensional shear band cleavage with down-to-the-north offset, north flank of Wiseman arch.

D_{1b}

D_{1b} structures and fabrics are pervasively developed throughout the metamorphic pile, and are by far the most common mesoscopic structural features in the schist belt. D_{1b} folds are close to isoclinal in geometry, and have wavelengths which range from less than a cm up to 0.5 m (Fig. 3b); they are commonly non-cylindrical, and individual fold axes may change in trend by as much as 40°. D_{1b} folds are associated with a penetrative axial planar crenulation cleavage (S_{1b}) which forms the dominant macroscopic planar fabric in the schist belt. S_{1b} and axial planes of D_{1b} folds dip mainly to the SE and E, but poles to S_{1b} are distributed in a NNW–SSE-trending girdle due to post-D_{1b} arching of the metamorphic pile (Figs. 2 and 5b & c). D_{1b} fold axes form a partial girdle distribution about the maximum of poles to axial planes, with a concentration in a N–S-trending orientation (Fig. 5b).

In isoclinally folded domains, S_{1b} is a penetrative composite planar fabric that resulted from transposition of S_{1a} (Tobisch & Paterson 1988) (Fig. 3c). Schistose rocks in areas of complete transposition commonly possess a well developed L–S tectonite fabric (Turner & Weiss 1963). S_{1a}/S_{1b} intersection lineations (L_{1b}) occur either as color bands on S_{1b} surfaces, or as prominent quartz rods where syn-D_{1a} quartz veins are folded. L_{1b} lineations parallel D_{1b} fold axes, and concentrate in a N–S-trending, subhorizontal orientation (Fig. 5d).

Microscopically, the morphology of S_{1b} is directly related to the geometry of associated folds. In domains where folds with close to tight geometries predominate, S_{1b} is mainly a zonal crenulation cleavage (Gray 1977); here, microlithon boundaries are diffuse and gradational, and coincide with microfold limbs (Fig. 6b). Where D_{1b} folds are tight to isoclinal, S_{1b} is predominantly a discrete crenulation cleavage (Gray 1977), defined by sharp discontinuities at microlithon boundaries (Fig. 6c). Although one cleavage morphology tends to dominate in any given fold, both discrete and zonal cleavage types are normally present; cleavage morphologies grade from one to the other both laterally and longitudinally.

Microstructural relations indicate that the differentiated crenulation cleavage (S_{1b}) in schistose rocks formed by a process involving microfolding of S_{1a}, dissolution and mass transfer of material, and nucleation and growth of new grains (cf. Cosgrove 1976, Gray 1977, Marlow & Etheridge 1977, Gray & Durney 1979, Bell & Rubenach 1983, Swager 1985). Dissolution of pre-D_{1b} minerals and concentration of insoluble residues occurred mainly along microfold limbs, forming curviplanar solution seams at microlithon boundaries. Solution seams also served as sites for the growth of

oriented neoblasts of phengite, paragonite, chlorite, and chloritoid in mica-rich schists; D_{1a} minerals are often entirely replaced, except for relicts preserved in D_{1b} fold hinges.

In quartz–mica schists, differentiation into quartz-rich (Q) and mica-rich (M) domains is common. In Q-domains, quartz occurs in polygonal-granoblastic aggregates, with individual quartz grains displaying undulatory extinction and local subgrain development; in M-domains, quartz grain shapes are defined by bounding mica grains. While structures such as undulatory extinction and subgrain development in quartz indicate deformation by dislocation slip and recovery (White 1973), it is not clear whether these features occur in the schist belt because the rate of dislocation generation exceeded the recovery rate during D_{1b}, or whether they are products of post-D_{1b} deformation. In either case, quartz in pelitic and semi-pelitic schists possesses a strong lattice-preferred orientation which corresponds to mesoscopic D_{1b} fabrics (Fig. 2), suggesting that quartz lattice-preferred orientations and D_{1b} fabrics are cogenetic. This relationship indicates that a significant portion of the strain produced during D_{1b} was accommodated by dislocation slip in quartz, in addition to the microfolding and dissolution-mass transfer mechanisms described above.

Snowball albite porphyroblasts containing S_{1b} graphitic inclusion trails are common in many samples of pelitic schist, semi-pelitic schist and albite schist (Fig. 6d). Their widespread distribution throughout the metamorphic pile attests to the importance of non-coaxial deformation in producing D_{1b} structures in the schist belt.

D_{1c}

D_{1c} folds are areally restricted to the northern flank of the Wiseman arch, where they occur in proximity to the Minnie Creek thrust and the Skajit décollement. Geometrically, D_{1c} structures are N-vergent, moderate to close folds (Fig. 3d) with S-dipping to sub-horizontal axial planes and E–W-trending, sub-horizontal fold axes (Fig. 5e). D_{1c} folds are locally associated with minor thrust faults along which top-to-the-north offset has occurred (Fig. 7). Dynamic analysis of rare D_{1c} conjugate fold sets indicates that the axis of shortening was N–S and sub-horizontal. These relations suggest that D_{1c} folds are related to N-directed thrusting, either along the Minnie Creek thrust, or along faults that formed during duplexing beneath the Skajit décollement.

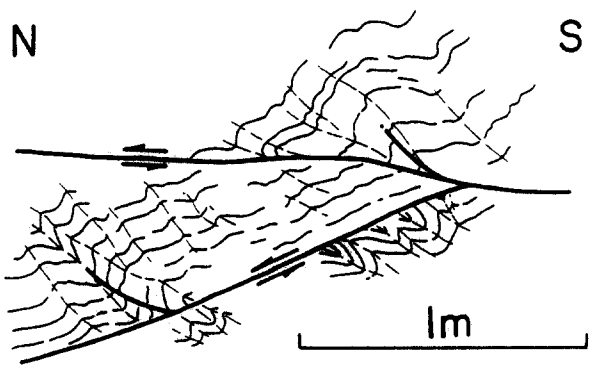

Fig. 7. Line drawing from photograph of D_{1c} folds and thrusts near northern structural boundary of schist belt.

A penetrative axial-planar cleavage (S_{1c}), and a prominent E–W-trending crenulation–intersection lineation (L_{1c}) are occasionally developed in association with D_{1c} folds. On a microscopic scale, S_{1c} occurs in irregular domains of both zonal and discrete cleavage morphologies. Microlithon boundaries in discrete cleavage domains serve as the site for limited growth of chlorite and white mica grains, dissolution of pre-D_{1c} quartz and mica grains, and concentration of insoluble residues. Within microlithons, quartz occurs in dilatant D_{1c} microfold hinges in a 'saddle reef' configuration; in rare cases, albite porphyroblasts enclose tiny D_{1c} crenulations. These relations indicate that limited growth of white mica, chlorite, quartz and albite was concurrent with, and possibly post-dated D_{1c}.

Deformation microstructures produced in quartz during D_{1c} are indicative of deformation by dislocation slip and recovery processes. Quartz grains in syn-D_{1b} segregations exhibit undulatory extinction and local subgrain development; where D_{1c} folding is most intense, quartz grains are composed entirely of subgrains, and are often surrounded by tiny strain-free neoblasts (i.e. core–mantle structures of White 1976). The persistent strength of quartz *c*-axis fabrics formed during D_{1b} suggests either that finite strains associated with D_{1c} were insufficient to significantly alter quartz lattice orientations, or that stress fields during D_{1b} and D_{1c} were similarly oriented. In the latter case, lattice-preferred orientations formed during D_{1b} may have been strengthened during D_{1c} folding.

Syn-D_{1c} *'static' recrystallization*

Throughout the metamorphic pile, D_{1a} and D_{1b} fabrics are overgrown and replaced by randomly oriented greenschist facies metamorphic minerals. In mica-rich schists, grains and sheaves of white mica and chlorite that cross-cut D_{1b} folds and fabrics are common (Fig. 6b), as are albite porphyroblasts which helicitically enclose D_{1b} structures. Foliated metabasites are often dominated by randomly oriented subidioblastic epidote porphyroblasts up to 15 mm in length (Fig. 6e). Xenoblastic albite and calcite porphyroblasts that cross-cut and enclose the planar fabric are also common in foliated metabasites (Fig. 6e), as are randomly oriented flakes of chlorite, biotite and stilpnomelane.

Several lines of evidence indicate that mineral growth under apparently 'static' conditions is, in fact, a dynamic phenomenon related to D_{1c} deformation. (1) Randomly oriented grains of white mica and chlorite are clearly corroded along D_{1c} dissolution seams, but in other cases overgrow dissolution seams and cross-cut D_{1c} fold hinges; this relationship indicates that 'static' recrystallization occurred during, and possibly following the formation of D_{1c} folds. (2) White mica grains that cross-cut S_{1b} at high angles often contain sigmoidal inclusion trails indicative of rigid-body rotation during growth. (3) In a

number of samples, S_{1b} wraps around post-D_{1b} epidote, albite and white mica grains, indicating minor layer-normal flattening following the growth of post-D_{1b} mineral grains. (4) In pelitic schists, strain shadows are formed around white mica grains which cross-cut S_{1b} at a high angle.

D_2

D_2 folds, ranging from a few cm to hundreds of meters in wavelength, occur throughout the metamorphic pile, and slightly re-orient earlier folds and penetrative fabrics. D_2 structures are predominantly S-vergent folds, with moderate to steeply N-dipping axial planes, and E–W-trending, sub-horizontal fold axes (Fig. 5g). South-vergent folds are locally associated with a N-dipping thrust fault along which minor S-directed offset has occurred. Where D_2 folds are gentle in geometry, they are symmetrical in cross-section, and have sub-vertically oriented E–W-striking axial planes.

D_2 folds in the schist belt are similar in geometry and orientation to S-vergent folds which are regionally developed throughout the central Brooks Range south of the Doonerak window (Phelps 1987, Handschy 1988, Boler 1989, Julian 1989, Seidensticker in preparation). Although the temporal relationship between D_2 and D_{1c} folds in the schist belt could not be determined from superposition relationships, the authors cited above have shown that S-vergent folds in the central Brooks Range post-date the formation of all N-vergent fold phases. Based on these relations, it is inferred that S-vergent folds in the schist belt post-date N-vergent D_{1c} folds, and are therefore designated D_2.

Extensional shear bands

East–west-striking extensional shear bands (Platt & Vissers 1980) occur sporadically throughout the metamorphic pile. South-dipping shear bands with down-to-the-south offset are most common, and occur on the southern flank and culmination of the Wiseman arch; N-dipping shear bands with down-to-the-north offset are restricted to the northern flank of the Wiseman arch (Fig. 5i). The relative ages of N- vs S-dipping shear bands could not be ascertained, but both exhibit similar structural styles and microstructural character. Morphologically, shear bands cross-cut the composite D_{1a}/D_{1b} fabric at low angles, terminating where they tangentially sweep into S_{1a}/S_{1b} (Fig. 3e). Shear bands do not exceed 30 cm in length and have measurable offsets restricted to a maximum of several cm. Due to their sporadic development in the schist belt, their timing relative to D_{1c} or S-vergent D_2 folding could not be determined from superposition relationships. In several pelitic schist samples, shear bands cross-cut randomly oriented, syn-D_{1c} (?) white mica and chlorite grains, suggesting that the formation of extensional shear bands may post-date D_{1c} folding.

In thin section, shear bands are zones of reduced grain size, composed of strain-free quartz and oriented neoblasts of chlorite and white mica (Fig. 6f). Individual shear bands are made up of a series of anastomosing microscopic shear zones that are spatially associated with minor conjugate shears (Fig. 8). Corrosion of quartz and mica grains along shear band surfaces indicates that dissolution–mass transfer processes played an important role in their formation. These relations suggest that shear bands are zones of localized strain softening in which dynamic recrystallization of quartz and dissolution–mass transfer processes were the chief deformation mechanisms. Although deformation took place at temperatures sufficient to allow dislocation slip and recovery processes to operate in quartz, the metamorphic grade associated with formation of extensional shear bands is uncertain.

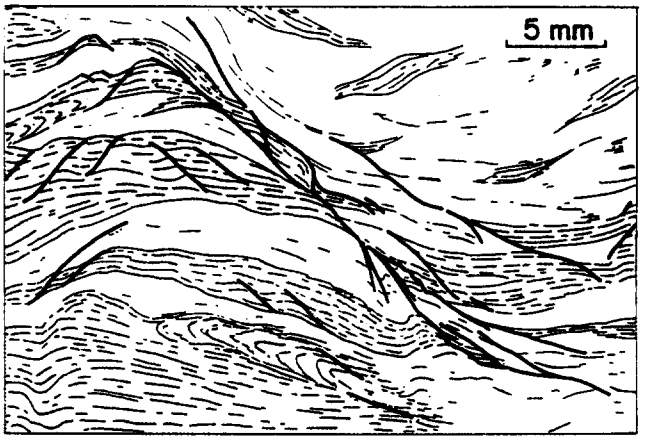

Fig. 8. Line drawing from thin section of a post-D_{1b} extensional shear band and subsidiary structures in pelitic schist. Shaded regions, mica-rich domains; unshaded regions, quartz-rich domains. Note that shear zones cross-cut D_{1b} isoclinal folds.

D_3

The youngest folds which affect the schist belt are a series of broad, map-scale flexures with N–S-trending fold axes and near-vertical, N–S-striking axial planes (Fig. 5j). Mesoscopic D_3 folds are rare, and occur as gentle buckle folds a few cm in wavelength. D_3 folds gently reorient D_{1a}, D_{1b}, D_{1c} and D_2 structures, but the relationship of D_3 folds to the extensional shear bands is unknown.

DISCUSSION

The schist belt, the Devonian metagreywacke belt, the phyllite belt, and Devonian (?) rocks in the southern Skajit allochthon, share a history of polyphase deformation and metamorphism. All are affected by superposed fold phases which, when contrasting lithologies and differing metamorphic grades are taken into account, are similar in style and orientation (Gottschalk 1987, and unpublished data). Mesoscopic structures developed throughout the south-central Brooks Range are thus post-Devonian in age. Since the Brooks Range is a site of relative tectonic quiescence from the Late

Devonian through Middle Jurassic (Mull 1982), it is probable that all of the penetrative structures developed in the central Brooks Range schist are post-Middle Jurassic in age. This is supported by textural and microstructural relationships, described in this paper, which indicate that the earliest recognizable structures in the central Brooks Range schist belt (D_{1a}) formed under glaucophane-stable conditions, probably during Late Jurassic to Early Cretaceous (?) *HP–LT* regional metamorphism.

D_{1a}, D_{1b} *and* D_{1c}

Although the kinematics of D_{1a} are difficult to determine, the widespread occurrence of sheath folds in the schist belt suggests that D_{1a} structures and fabrics formed in a non-coaxial strain regime (Quinquis *et al.* 1978, Cobbold & Quinquis 1980). Quinquis *et al.* (1978) and Cobbold & Quinquis (1980) have also shown that in bodies of rock subjected to high shear strains, the axes of sheath folds and associated isoclinal folds lie approximately parallel to the direction of tectonic transport. The N–S trend of D_{1a} fold axes, as deduced from interference patterns with D_{1b} folds, indicates that the tectonic transport during D_{1a} was either N- *or* S-directed. The sense of shear during D_{1a} could not be determined due to intense post-D_{1a} deformation and recrystallization.

Structural analysis of D_{1b} structures and fabrics indicates that they are products of a non-coaxial strain regime dominated by top-to-the-north shear. The dominance of syn-D_{1b} shear throughout the entire structural thickness of schist belt is indicated by the widespread occurrence of snowball albite and garnet porphyroblasts. In thin sections cut perpendicular to S_{1b} and parallel to N–S-trending D_{1b} fold axes, vorticities of synkinematic albite and garnet porphyroblasts indicate a top-to-the-north shear sense in six out of seven oriented samples which contain shear sense indicators.

Quartz petrofabrics support conclusions drawn from microstructural relations. The *c*-axes of quartz grains dynamically recrystallized during D_{1b} generally form type-I cross-girdle fabrics (Lister 1977) with a marked degree of asymmetry with respect to the foliation plane (Fig. 2). Fabrics of this type are common in quartz-rich tectonites subjected to high shear strains, and numerous studies have shown that the inclination of the girdle with respect to the foliation plane reflects the sense of shear (Lister & Williams 1979, Bouchez *et al.* 1983, Price 1985, Schmid & Casey 1986). Of nine samples whose quartz *c*-axes display asymmetric fabrics, eight indicate a top-to-the-north shear sense, supporting the microstructural evidence cited above. In cases where syn-kinematic porphyroblasts occur in the same sample whose quartz *c*-axes were measured, shear senses are the same. The quartz fabric shown in Fig. 2(a), however, is essentially symmetrical with respect to the foliation plane, suggesting that bulk strain in the schist belt may have been partitioned into domains of simple shear and localized coaxial strain. Note also that quartz fabrics from one sample (Fig. 2h) indicate a top-to-the-south shear sense. Domains in which the local shear sense opposes that of the dominant sense of shear have been reported from other ductile movement zones (Eisbacher 1970, Bouchez & Pecher 1981, Garcia-Celma 1982, Lacassin 1987), and indicate a local deviation from bulk simple shear in the deforming medium. Possible causes for local reversal of shear sense in the schist belt are unknown.

Quartz petrofabric analysis also provides constraints on the state of finite strain in the schist belt, and on the relationship between finite strain and D_{1b} fabric elements. Axes of tight to isoclinal D_{1b} folds and L_{1b} lineations correspond to the pole-free area of quartz *c*-axis diagrams (Fig. 2). Theoretical models (Lister & Hobbs 1980), studies on experimentally deformed quartz-rich aggregates (Tullis *et al.* 1973, Tullis 1977), and numerous studies of quartz-rich rocks in naturally occurring shear zones indicate that, in rocks deformed at temperatures below approximately 650°C (Mainprice *et al.* 1986), the pole-free area of *c*-axis diagrams corresponds approximately to the *X*-axis of finite strain ($X \geq Y \geq Z$). Thus, in samples where quartz fabrics were measured, D_{1b} fold axes and lineations are approximately parallel to the *X*-axis of finite strain, and are all N–S and subhorizontal.

The parallelism of fold axes to the *X*-axis of finite strain has been explained by many authors (e.g. Bryant & Reed 1969, Sanderson 1973, Escher & Watterson 1974, Bell 1978) as the result of passive rotation of fold axes into *X* during progressive shear deformation; as fold axes rotate toward *X*, *X* asymptotically rotates into the orientation of the shear couple. Thus, with sufficiently large shear strains, fold axes and lineations will form a point maximum subparallel to both the *X*-axis of finite strain and the direction of tectonic transport. The N–S trend of D_{1b} fold axes, L_{1b} lineations, and the *X*-axis of finite strain in the schist belt indicate that, during D_{1b}, the transport direction lay in a N–S orientation. Material transport occurred in a thick zone within which top-to-the-north shear predominated.

The N-vergent geometry of D_{1c} folds, their relationship to minor thrust faults with top-to-the-north offset, and the concentration of D_{1c} folds in the vicinity of faults along the northern boundary of the schist belt, indicate that D_{1c} folds formed during N-directed emplacement of the schist belt along the Minnie Creek thrust, or during N-directed offset along thrust faults related to duplexing beneath the Skajit décollement. Strains were sufficiently low in areas away from thrust faults that greenschist facies metamorphic minerals grew in an unconstrained fashion, producing the apparently 'static' overgrowth which affects rocks in the schist belt.

Kinematic model for D_{1a}, D_{1b} *and* D_{1c}

Several lines of evidence suggest that D_{1a}, D_{1b} and D_{1c} folds are products of a single event of syn-metamorphic progressive deformation. (1) All three fold phases must have formed over a limited time period prior to the late Early Cretaceous emergence of the

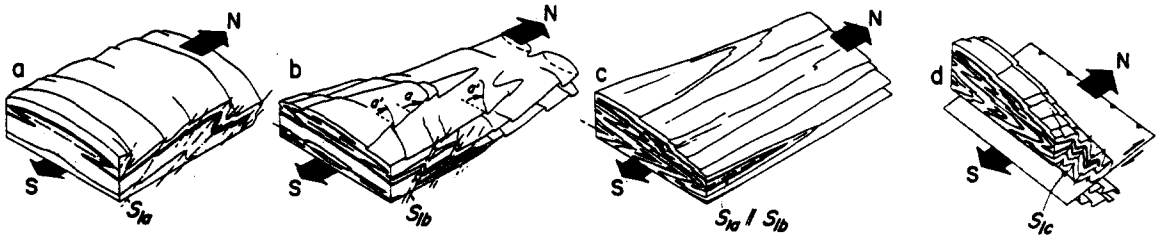

Fig. 9. Model for the evolution of synmetamorphic structures in schist belt. (a) Nucleation of D_{1a} folds during early stages of top-to-the-north shear deformation. With continued deformation: (b) D_{1a} fold axes become increasingly arcuate (i.e. angle a increases) and axial planes rotate into the shear plane during continued deformation; D_{1a} sheath folds and isoclines with axes approximately parallel to the shear direction are produced. D_{1b} folds nucleate with axes at a high angle to the direction of tectonic transport. D_{1a} and D_{1b} fold axes both rotate into the transport direction (angles a and a' increase) and S_{1b} axial planes rotate into the shear plane. The coaxial and coplanar fabric shown in (c) is the end result. (d) Formation of D_{1c} folds in zone of high cumulative strain near thrust fault.

schist belt, recorded by numerous K–Ar and Rb–Sr age dates which cluster around 100–130 Ma (Brosgé & Reiser 1964, Turner *et al.* 1979, Armstrong *et al.* 1986), and by the presence of *HP–LT* metamorphic detritus in Albian–Cenomanian sediments of the foredeep succession (Till 1988). (2) The geometries and inferred kinematics of all three fold phases are consistent with formation in a strain regime dominated by top-to-the-north shear, and a stress regime dominated by N–S, subhorizontal compression. (3) There is no textural evidence for interkinematic mineral growth between D_{1a}, D_{1b} and D_{1c} fold phases, suggesting that folds were nucleating and growing continuously.

Whereas D_{1a} folds formed under glaucophane-stable metamorphic conditions, textural relations suggest that rocks of the schist belt were dynamically recrystallized under greenschist facies conditions during D_{1b} and D_{1c}. If D_{1a} structures formed at metamorphic pressures similar to peak pressure conditions recorded in the Seward Peninsula blueschist (9–12 kbar, from Forbes *et al.* 1984, Thurston 1985, Evans & Patrick 1987), then rocks of the schist belt may have been metamorphosed at depths as great as 40 km, and uplifted to moderate pressure greenschist facies metamorphic conditions during N–S-directed compressional deformation; a thermobarometric study now in progress, will help to quantify the magnitude of syn-compressional uplift of the schist belt.

The following kinematic model is proposed to explain the formation of superposed syn-metamorphic folds during progressive shear deformation. Protracted top-to-the-north shear, concurrent with *HP–LT* regional metamorphism in the schist belt, resulted in the nucleation of D_{1a} folds. Continued deformation caused arcuation of D_{1a} fold axes, and rotation of D_{1a} axial planes into the shear plane (Fig. 9a); fold axes continued to rotate toward the direction of tectonic transport, ultimately forming sheath folds and isoclinal folds with dominantly N–S-trending axes. As rocks were being uplifted to shallower structural levels, D_{1b} folds began to nucleate, perhaps in response to perturbations in the flow field caused by ductility contrasts created during D_{1a} (Lister & Williams 1983, Platt 1983, Ghosh & Sengupta 1984) (Fig. 9b). As deformation progressed, D_{1b} folds continued to nucleate, D_{1b} axial planes rotated into the shear plane, and the axes of D_{1a} and D_{1b} folds continued their rotation into the northerly direction of tectonic transport. The coaxial and coplanar geometry of D_{1a} and D_{1b} folds indicates that shear strains were sufficiently large to rotate both generations of fold axes into the direction of tectonic transport, and into parallelism with one another (Fig. 9c). Finally, D_{1c} folds formed in a zone of locally higher cumulative strain near thrust-faults (Fig. 9d).

D_2

Folds with S-vergent asymmetry, associated with minor S-directed thrusting, indicate that the schist belt has been affected by a relatively late-stage event of top-to-the-south shear. As with D_{1a}, D_{1b} and D_{1c} structures, D_2 folds are consistent with formation in a stress regime dominated by N–S subhorizontal compression, suggesting that D_2 folds may also be a product of progressive deformation. Possible explanations for the reversal in tectonic transport direction from D_{1a}, D_{1b} and D_{1c} to D_2 are discussed below.

Extensional shear bands

The geometry and orientation of extensional shear bands indicates that they formed during a period of N–S extension that post-dates the formation of compressional structures in the schist belt. The spatial distribution of N- and S-dipping extensional shear bands on the northern and southern flanks of the Wiseman arch, respectively, also suggest that their origin may be related to the arch structure. Uncertainties regarding the relative timing of thrusting, arching of the metamorphic pile, and the formation of shear bands does not allow for a unique interpretation for the origin of shear bands. Several possibilities exist: (1) N–S extension may have occurred by homogeneous stretching of a pre-existing arch-structure (i.e. the Wiseman arch may have formed prior to extension as a hangingwall anticline above the Minnie Creek thrust). If the formation of extensional shear bands was facilitated by intrafolial slip in the metamorphic pile, then S-dipping shear bands would be expected to predominate on the southern flank of the Wiseman arch (Fig. 10a); (2) shear bands may have formed in response to differential uplift or differential

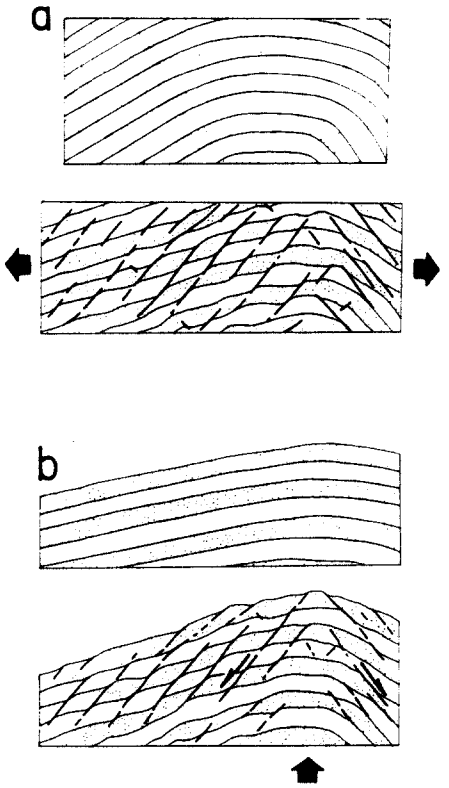

Fig. 10. Models for extensional structures produced by (a) homogeneous stretching of a pre-existing foliation arch; (b) extensional collapse or uplift centered on axis of pre-existing structural culmination.

collapse centering on the axis of the Wiseman arch (Fig. 10b). If the Wiseman arch was created solely during N–S compression, then extensional shear bands may be accommodation structures related to thrust sheet emplacement (Fig. 11). Alternatively, differential collapse and uplift may be related to regional extension about a structural culmination that was produced during an earlier thrusting event; Brown & Journeay (1986) describe such a relationship in the Shuswap metamorphic complex of British Columbia, where extension appears to have occurred mainly on the flanks of older compressional structural culminations.

D_3

The N–S strike and vertical orientation of the axial planes of gentle D_3 warps are indicative of E–W shortening which post-dated the N–S compression associated with D_{1a}, D_{1b}, D_{1c} and D_2. The relative timing of E–W compression to N–S extension in the schist belt is unknown.

TECTONIC IMPLICATIONS

Subduction phase (Late Jurassic–Early Cretaceous)

HP–LT metamorphic belts involving continental rocks are exposed in many collisional orogens, including the Alps (e.g. Chopin 1984, Dal Piaz & Lombardo 1986, Koons 1986, Pognante *et al.* 1987), the Betic Cordillera, Spain (Gomez-Pugnaire & Fernandez-Soler 1987), the Cycladic belt, Greece (Matthews & Schliestedt 1984), Turkey (Okay 1986) and Oman (Goffé *et al.* 1988). In these orogens, *HP–LT* metamorphism is believed to result from the subduction of continental crust or crustal fragments beneath an impinging continental landmass or an island-arc edifice. Structural and metamorphic relations in the Brooks Range suggest that early penetrative structures in the schist belt (D_{1a}) may have formed in an analogous tectonic setting: during D_{1a}, the schist belt experienced intense top-to-the-north shear deformation concurrent with *HP–LT* metamorphism; these relations are compatible with formation of D_{1a} structures during S-directed subduction (in present-day co-ordinates) of the Arctic Alaskan microplate beneath the Yukon–Koyukuk arc, Angayucham terrane, and allochthonous metasedimentary rocks (Fig. 12b). Subduction probably occurred in Late Jurassic–Early Cretaceous time (Armstrong *et al.* 1986).

Contractional phase (Early Cretaceous)

Structural and metamorphic relations that suggest uplift during N–S, subhorizontal compression are consistent with the involvement of the schist belt and subjacent crustal rocks in N-directed thrusting, as shown in Fig. 12. The top-to-the-north shear that created D_{1b} folds within basement thrust sheets probably occurred when rocks now exposed at the surface were at structural levels sufficiently deep to allow pervasive ductile deformation and dynamic recrystallization to take place; it is possible that D_{1a} structures may have formed, in part, during the thrusting rather than subduction phase of tectonism. D_{1c} folds are late-stage features that formed as basement thrust sheet(s) continued to move to shallower structural levels, and northward with respect to autochthonous basement.

Structural relations thus support the thin-skinned interpretation for the structure of the Brooks Range fold and thrust belt favored by Gottschalk (1987), Oldow *et al.* (1987a), Gottschalk & Oldow (1988) and Till *et al.* (1988). In the opinion of these authors, the schist belt is an allochthonous structural entity, separated from autochthonous basement by a low-angle thrust fault; this basal structure is presumed to be a portion of a regional décollement surface which continues northward beneath the foreland of the fold and thrust belt. Given this

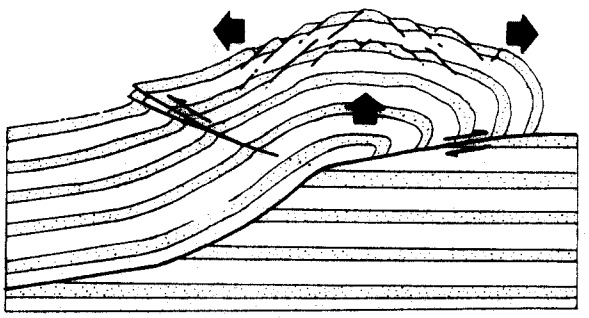

Fig. 11. Diagram showing possible structural relationship between compressional and extensional structures in the schist belt.

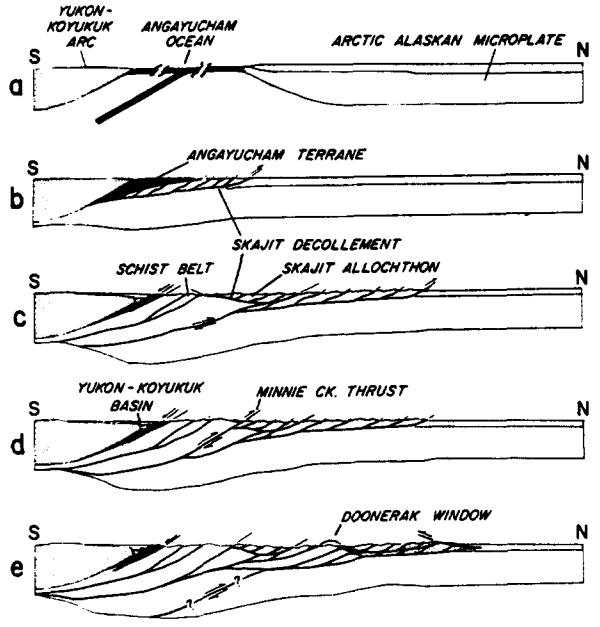

Fig. 12. Schematic cross-sections showing possible mechanics of deformation in hinterland of the central Brooks Range fold and thrust belt (based on reconstructions of Oldow *et al.* 1987a). Actual amounts of uplift related to duplexing beneath the Skajit décollement and Skajit allochthon vs offset on the Minnie Creek thrust are not known. Stipple pattern, Lower Paleozoic (?) and younger metasedimentary rocks. Unornamented, basement of Arctic Alaskan microplate, including schist belt. See text for explanation.

geometry, the structural and metamorphic history of the schist belt has a number of tectonic ramifications of regional importance.

(1) Structures in the schist belt record the transition from S-directed subduction of the Arctic Alaskan microplate to N-directed thrust faulting involving previously subducted rocks. The cessation of subduction probably resulted from resistance to underthrusting due to buoyancy of the continental crust; continued N–S contraction was presumably transferred to S-dipping thrust-faults which involved the basement of the Arctic Alaskan microplate (Fig. 12c). Oldow *et al.* (1987a) suggest that shortening within the basement was taken up by crustal duplexing beneath the Skajit allochthon.

(2) In the schist belt, rocks which may have been metamorphosed at depths as great as 40 km are presently exposed at the surface. If uplift of the schist belt was accomplished in large part by thrust faulting, then the basal décollement in the hinterland of the central Brooks Range must have been located deep within the continental crust, as shown in Fig. 12.

(3) Syn-compressional uplift of the schist belt probably resulted from a process involving simultaneous ramping of basement thrust sheets along S-dipping thrust faults, and isostatic uplift due to crustal thickening in the hinterland (Figs. 12c, d & e). Metamorphic decompression in the schist belt requires that uplift was accompanied by significant erosion and (or) tectonic thinning of cover rocks.

(4) Constraints on the geometry of thin-skinned fold and thrust belts require that shortening taken up in the foreland be transferred to thrust faults which involve deep crustal rocks in the hinterland. Given that shortening in the foreland of the Brooks Range took place through the Eocene and possibly later, imbrication of continental basement and resultant uplift of hinterland may have been a continuous process which spanned from Late Jurassic–Early Cretaceous to Early Tertiary and possibly later time.

Retrocharriage (age uncertain)

Regionally developed S-vergent folds (D_2) are present throughout the central Brooks Range south of the Doonerak Window. Mull (1982) has suggested that S-vergent folds may have formed by partial N-directed underthrusting of the Yukon–Koyukuk island-arc and Angayucham terrane beneath the previously imbricated continental margin sediments of the Brooks Range; in Mull's model, S-vergent folds post-date the formation of N-vergent structures. Alternatively, Seidensticker *et al.* (1987) contend that the Doonerak window duplex may have acted as an impediment to slip along the basal décollement of the fold and thrust belt, resulting in homogeneous shortening south of the Doonerak window by formation of S-vergent folds. If the Doonerak window duplex is a relatively late-orogenic feature (Oldow *et al.* 1987a), the S-vergent folding in the southern Brooks Range must have post-dated the formation of N-vergent structures (D_{1a}, D_{1b} and D_{1c}) in the schist belt (Fig. 12e). The models of Mull (1982) and Seidensticker *et al.* (1987) predict identical structural sequences, and both are compatible with the polyphase structures in the schist belt.

Extensional phase (Early to Mid-Cretaceous ?)

Recent studies in the Brooks Range cite evidence for N–S extension that has significantly altered the distribution of allochthonous rocks in the hinterland of the Brooks Range (Gottschalk 1987, Oldow *et al.* 1987b, Box 1987, Miller 1987, Gottschalk & Oldow 1988, Harris 1988, Avé Lallemant *et al.* 1989, Christiansen 1989). In the south-central Brooks Range, Gottschalk & Oldow (1988) have argued that low metamorphic grade over high metamorphic grade structural relations along the southern flank of the schist belt resulted from extensional offset along S-dipping normal faults. Their contentions are supported by the recent work of Avé Lallemant *et al.* (1989) who demonstrated that the allochthons which structurally overlie the schist belt (the metagreywacke belt and Angayucham terrane) have been internally distended along numerous mesoscopic faults; structural analysis of these small-scale faults indicates that they formed during a period of N–S extension. The geometry and orientation of ductile extensional shear bands in the schist belt are also consistent with formation during N–S extension in the southern Brooks Range. These relationships suggest that the period of extension during which brittle faults were produced in the metagreywacke belt and Angayucham terrane also

produced ductile extensional structures in the schist belt.

The age of extension in the south-central Brooks Range is, at present, poorly constrained. Along the northern boundary of the Ruby Geanticline (Fig. 1), however, a granitic pluton dated at 112 ± 4 Ma (Blum *et al.* 1987) intrudes faults which place oceanic rocks of the Angayucham terrane and low-grade metasedimentary rocks above relatively high-grade metamorphics. This structural configuration is essentially identical to that argued by Gottschalk & Oldow (1988) to be the result of N–S extension in the Brooks Range. Thus within the resolution of current data, regional relations indicate that extension in central Alaska, including the southern Brooks Range, had ceased by Albian time. Although age of inception of extension in central Alaska is not known, extant chronologic data and regional geologic relationships are consistent with models in which late Early Cretaceous uplift of the schist belt is accommodated by tectonic denudation and thinning of cover rocks along extensional faults (Gottschalk 1987, Box 1987, Miller 1987, Oldow *et al.* 1987b, Gottschalk & Oldow 1988, Avé Lallemant *et al.* 1989).

Contractional structures in the Brooks Range and North Slope are believed to range from Late Jurassic–Early Cretaceous (Mayfield *et al.* 1983) to Eocene and possibly younger in age (Hubbard *et al.* 1987, Oldow *et al.* 1987a). If compressional deformation was continuous over this period, then extension in the southern Brooks Range took place within the contractional Brooks Range orogen. The apparent paradox of simultaneous extension and compression within the same deformational belt can be explained by a mechanism similar to that proposed by Platt (1986), wherein compressional uplift of *HP–LT* metamorphic rocks is accommodated by the formation of extensional structures at shallow structural levels. In the Brooks Range, local tensile stresses at shallow structural levels in the hinterland of the fold and thrust belt may have resulted from disruption of the critical taper of the imbricate stack, caused by extreme crustal thickening. Thus, the change in the local stress field from N–S compression to N–S extension may have occurred as the schist belt was uplifted to shallower structural levels where local extension was occurring in response to oversteepening of the imbricate stack. The temporal relationship between N–S extension and the formation of S-vergent folds (D_2) is not known.

East–west compression (Late Cretaceous ?)

The Angayucham terrane, metagreywacke belt, phyllite belt, and the schist belt are all affected by a series of gentle folds and broad scale warps (D_3) indicative of E–W compression. The 90° shift in the orientation of compressive stress from N–S to E–W may have resulted from the onset of differential movement between the Siberian and Arctic Alaskan portions of the North American plate in the Late Cretaceous (Patton & Tailluer 1977, Harbert *et al.* 1987).

SUMMARY AND CONCLUSIONS

Polyphase folds in the schist belt of the central Brooks Range record a complex structural and metamorphic history which can be related to: (1) Late Jurassic–Early Cretaceous collision between the Yukon–Koyukuk island-arc and the passive continental margin of the Arctic Alaskan microplate; (2) Cretaceous and younger contractional tectonism in the Brooks Range fold and thrust belt; (3) late Early Cretaceous extension; and (4) Late Cretaceous (?) compression possibly related to differential movement between the Alaskan and Siberian portions of the North American plate.

(1) *Subduction phase (Late Jurassic–Early Cretaceous)*

The oldest structures in the schist belt (D_{1a}) are isoclinal folds and sheath folds with N–S-trending fold axes. Although present throughout the metamorphic pile, D_{1a} folds are sporadically preserved due to the intensity of later folding and recrystallization. Textural and microstructural relations indicate that D_{1a} structures and fabrics formed under glaucophane-stable metamorphic conditions. The geometries and orientations of D_{1a} structures are consistent with formation during S-directed subduction (in present-day coordinates) of the Arctic Alaskan continental microplate beneath the Yukon–Koyukuk island-arc, Angayucham terrane, and continental metasediments in the Late Jurassic–Early Cretaceous.

(2) *Contractional phase (Early Cretaceous)*

D_{1a} structures are refolded by a second phase of syn-metamorphic folds (D_{1b}) with close to isoclinal geometries and N–S-tending fold axes. During D_{1b}, the entire exposed structural thickness of the schist belt was subjected to top-to-the-north shear, and dynamically recrystallized under greenschist facies metamorphic conditions. The inferred strain regimes and deformational kinematics for D_{1a} and D_{1b} are nearly identical, suggesting that both fold phases formed during a single event of N–S compression. However, the replacement of syn-D_{1a} *HP–LT* metamorphic assemblages by greenschist facies assemblages during D_{1b} suggests that significant uplift occurred during progressive deformation. These relations are interpreted to reflect the involvement of previously subducted rocks in N-directed thrusting, resulting in uplift of *HP–LT* metamorphics along S-dipping thrust faults, and generation of N-vergent syn-metamorphic D_{1b} folds within the thrust sheets. D_{1c} folds are N-vergent folds that occur only in the vicinity of thrust faults along the northern boundary of the schist belt; they record the final emplacement of formerly deep-seated metamorphic rocks along thrust faults.

The cessation of continental subduction probably resulted from buoyant resistance to underthrusting beneath the Yukon–Koyukuk arc and Angayucham terrane. Continued N–S contraction was presumably transferred to south-dipping thrust faults which involved the

basement of the Arctic Alaskan microplate; thrust faults may have penetrated to depths of 40 km or greater. Shortening within the basement was presumably taken up by crustal duplexing beneath the Skajit allochthon (Oldow *et al.* 1987a).

South-vergent folds (D_2) which formed during continued N–S compression, occur throughout the central Brooks Range south of the Doonerak Window, and refold D_{1a}, D_{1b} and possibly D_{1c} structures in the schist belt. The change to S-directed tectonic transport during D_2 may be related to the onset of partial N-directed underthrusting of the Yukon–Koyukuk arc and Angayucham terrane beneath previously imbricated continental rocks (Mull 1982), or to the formation of the Doonerak Window duplex (Seidensticker *et al.* 1987).

(3) *Extensional phase (late Early Cretaceous)*

Extensional shear bands in the schist belt record a period of N–S ductile extension which post-dates the formation of thrust-related structures (i.e. post-D_{1b} and possibly post-D_{1c}). Ductile extensional structures in the schist belt are probably contemporaneous with brittle structures which extended the overlying metagreywacke belt and Angayucham terrane (Avé Lallemant *et al.* 1989).

Regional geologic relationships indicate that uplift of the schist belt and N–S extension in the southern Brooks Range were contemporaneous with contractional deformation elsewhere in the Brooks Range. These apparently paradoxical relationships may be explained by the model of Platt (1986), in which the compressional uplift of *HP–LT* metamorphic rocks is accommodated by the development of normal faults at shallow structural levels in the contractional orogen. In the central Brooks Range, the late Early Cretaceous uplift of the schist belt along S-dipping thrust faults was presumably accommodated by tectonic denudation and thinning of cover rocks along extensional faults. Compressional D_{1b} and D_{1c} structures may have been forming at depth in the schist belt at the same time that normal faults were extending the overlying allochthons. The temporal relationship between N–S extension and the formation of S-vergent folds (D_2) is not known.

(4) *East–west compressional phase (Late Cretaceous ?)*

D_3 folding in the schist belt resulted from E–W oriented compression, perhaps related to differential movement between the Siberian and Arctic Alaskan portions of the North American plate in the late Cretaceous (Patton & Tailluer 1977, Harbert *et al.* 1987).

Acknowledgements—Funding for this study was provided by grants from the Department of Energy (DE-ASO5-83ER13124), the National Science Foundation (EAR-8517384; EAR-8720171), and the Alaska Industrial Associates Program (AIAP) at Rice University and the University of Alaska, Fairbanks. The AIAP received contributions from Arco, Amoco, Chevron, Standard Oil of Ohio, Mobil, and Gulf. Critical reviews by L. H. Shapiro, R. L. Brown, A. B. Till, H. G. Avé Lallemant and J. S. Oldow significantly improved the quality of this manuscript.

REFERENCES

Armstrong, R. L., Harakal, J. E., Forbes, R. B., Evans, B. W. & Thurston, S. P. 1986. Rb–Sr and K–Ar study of metamorphic rocks of the Seward Peninsula and southern Brooks Range, Alaska. In: *Eclogites and Blueschists* (edited by Evans, B. W. & Brown, E. H.). *Mem. geol. Soc. Am.* **164**, 185–203.

Avé Lallemant, H. G., Oldow, J. S. & Gottschalk, R. R. 1989. Mesoscopic fault analysis in the south-central Brooks Range fold and thrust belt, Alaska. *Geol. Soc. Am. Abs. w. Prog.* **21**, 52.

Bell, T. H. 1978. Progressive deformation and reorientation of fold axes in a ductile mylonite zone: the Woodroffe thrust. *Tectonophysics* **44**, 285–320.

Bell, T. H. & Rubenach, M. J. 1983. Sequential porphyroblast growth and crenulation cleavage development during progressive deformation. *Tectonophysics* **92**, 171–194.

Blum, J. D., Blum, A. E., Davis, T. E. & Dillon, J. T. 1987. Petrology of cogenetic silica-saturated and -oversaturated plutonic rocks in the Ruby geanticline of north-central Alaska. *Can. J. Earth Sci.* **24**, 159–169.

Boler, K. B. 1989. Stratigraphy, structure, and tectonics of the central Brooks Range near Dietrich Camp, Alaska. Unpublished M.A. thesis, Rice University, Houston, Texas.

Bouchez, J.-L., Lister, G. S. & Nicolas, A. 1983. Fabric asymmetry and shear sense in movement zones. *Geol. Rdsch.* **72**, 401–419.

Bouchez, J.-L. & Pecher, A. 1981. The Himalayan main central thrust pile and its quartz-rich tectonites in central Nepal. *Tectonophysics* **78**, 23–50.

Box, S. E. 1985. Early Cretaceous orogenic belt in northwestern Alaska: internal organization, lateral extent, and tectonic interpretation. In: *Tectonostratigraphic Terranes of the Circum-Pacific Region* (edited by Howell, D. G.). Circum-Pacific Council for Energy and Mineral Resources, Houston, 137–145.

Box, S. E. 1987. Cretaceous or younger southwest-directed extensional faulting, Cosmos Hills, Brooks Range, Alaska. *Geol. Soc. Am. Abs. w. Prog.* **19**, 361.

Brosgé, W. P. & Reiser, H. N. 1964. Geologic map and section of the Chandalar quadrangle, Alaska. *U.S. Geol. Surv. Misc. Geol. Inv. Map* I-375, scale 1:250,000.

Brosgé, W. P. & Reiser, H. N. 1971. Preliminary bedrock geologic map: Wiseman and eastern Survey Pass quadrangles, Alaska. *U.S. Geol. Surv. Open File Map* 479, scale 1:250,000.

Brosgé, W. P., Reiser, H. N., Dutro, J. T. Jr. & Detterman, R. L. 1979. Bedrock geologic map of the Philip Smith Mountains quadrangle. *U.S. Geol. Surv. Misc. Field Studies Map* MF-879B, scale 1:250,000.

Brown, R. L. & Journeay, J. M. 1986. Tectonic denudation of the Shuswap metamorphic terrane of southern British Columbia. *Geology* **15**, 142–146.

Bryant, B. & Reed, J. C. 1969. Significance of lineation and minor folds near major thrust faults in the southern Appalachians and the British and Norwegian Caledonides. *Geol. Mag.* **106**, 412–429.

Chopin, C. 1984. Coesite and pure pyrope in high-grade blueschists of the western Alps: a first record and some consequences. *Contr. Miner. Petrol.* **86**, 107–118.

Christiansen, P. P. 1989. Cretaceous faulting and deformation in the Cosmos Hills, southern Brooks Range, Alaska. *Geol. Soc. Am. Abs. w. Prog.* **21**, 65.

Cobbold, P. R. & Quinquis, H. 1980. Development of sheath folds in shear regimes. *J. Struct. Geol.* **2**, 119–126.

Cosgrove, J. W. 1976. The formation of crenulation cleavage. *J. geol. Soc. Lond.* **132**, 155–178.

Dal Piaz, G. V. & Lombardo, B. 1986. Early Alpine eclogite metamorphism in the Penninic Monte Rosa-Gran Paradiso basement nappes of the northwestern Alps. In: *Eclogites and Blueschists* (edited by Evans, B. W. & Brown, E. H.). *Mem. geol. Soc. Am.* **164**, 249–263.

Dillon, J. T., Brosgé, W. P. & Dutro, J. T., Jr. 1986. Generalized geologic map of the Wiseman quadrangle, Alaska. *U.S. Geol. Surv. Open File Report* OF 86-219, scale 1:250,000.

Dillon, J. T., Pessel, G. H., Chen, J. H. & Veach, N. C. 1980. Middle Paleozoic magmatism and orogenesis in the Brooks Range, Alaska. *Geology* **8**, 338–343.

Dillon, J. T., Harris, A. G. & Dutro, J. T., Jr. 1987. Preliminary

description of Lower Paleozoic fossil-bearing strata in the Snowden Mountain area of south-central Brooks Range, Alaska. In: *Alaskan North Slope Geology* (edited by Tailluer, I. & Weimer, P.). *Spec. Publs Pacific Section, Soc. econ. Paleont. Miner.* **1**, 337–345.

Dutro, J. T., Jr, Brosgé, W. P., Lanphere, M. A. & Reiser, H. N. 1976. Geologic significance of Doonerak structural high, central Brooks Range, Alaska. *Bull. Am. Ass. Petrol Geol.* **60**, 952–961.

Dutro, J. T., Jr, Palmer, A. R., Repetski, J. E. & Brosgé, W. P. 1984. Middle Cambrian fossils from the Doonerak Anticlinorium, central Brooks Range, Alaska. *J. Paleont.* **58**, 1364–1371.

Eisbacher, G. H. 1970. Deformation mechanics of mylonite rocks and fractured granites in Cobequid mountains, Nova Scotia, Canada. *Bull. geol. Soc. Am.* **81**, 2009–2020.

Escher, A. & Watterson, J. 1974. Stretching fabrics, folds and crustal shortening. *Tectonophysics* **22**, 223–231.

Evans, B. W. & Patrick, B. E. 1987. Phengite (3T) in high-pressure metamorphosed granitic orthogneisses, Seward Peninsula, Alaska. *Can. Mineral.* **25**, 141–158.

Forbes, R. B., Evans, B. W. & Thurston, S. P. 1984. Regional progressive high-pressure metamorphism, Seward Peninsula, Alaska. *J. metamorph. Geol.* **66**, 113–117.

Garcia-Celma, A. 1982. Domainal and fabric heterogeneities in the Cap de Creus quartz mylonites. *J. Struct. Geol.* **4**, 443–455.

Ghosh, S. K. & Sengupta, S. 1984. Successive development of plane noncylindrical folds in progressive deformation. *J. Struct. Geol.* **9**, 277–287.

Goffé, B., Michard, A., Kienast, J.-R. & Le Mer, O. 1988. A case of obduction-related high-pressure, low-temperature metamorphism in upper crustal nappes, Arabian continental margin, Oman: P–T paths and kinematic interpretation. *Tectonophysics* **151**, 363–386.

Gomez-Pugnaire, M. T. & Fernandez-Soler, J. M. 1987. High-pressure metamorphism in metabasites from the Betic Cordilleras (S.E. Spain) and its evolution during the Alpine orogeny. *Contr. Miner. Petrol.* **95**, 231–244.

Gottschalk, R. R. 1987. Structural and petrologic evolution of the south-central Brooks Range, Alaska. Unpublished Ph.D. thesis, Rice University, Houston, Texas.

Gottschalk, R. R. & Oldow, J. S. 1988. Low-angle normal faults in the south-central Brooks Range fold and thrust belt, Alaska. *Geology* **16**, 395–399.

Gray, D. R. 1977. Some parameters which affect the morphology of crenulation cleavages. *J. Geol.* **85**, 763–780.

Gray, D. R. & Durney, D. W. 1979. Crenulation cleavage differentiation: implications of solution deposition processes. *J. Struct. Geol.* **1**, 73–80.

Handschy, J. W. 1988. Sedimentology and structural geology of the Endicott Mountains allochthon, central Brooks Range, Alaska. Unpublished Ph.D. thesis, Rice University, Houston, Texas.

Harbert, W., Frei, L. S., Cox, A. & Engebretson, D. C. 1987. Relative plate motions between Eurasia and North America in the Bering Sea region. *Tectonophysics* **134**, 239–261.

Harris, R. A. 1988. Origin, emplacement, and attenuation of the Misheguk Mountain allochthon, western Brooks Range, Alaska. *Geol. Soc. Am. Abs. w. Prog.* **20**, A112.

Hitzman, M. W., Proffett, J. M., Schmidt, J. M. & Smith, T. E. 1986. Geology and mineralization of the Ambler district, northwestern Alaska. *Econ. Geol.* **91**, 1592–1618.

Hubbard, R. J., Edrich, S. P. & Rattey, R. P. 1987. Geologic evolution and hydrocarbon habitat of the Arctic Alaskan microplate. *Mar. Petrol. Geol.* **4**, 2–34.

Jones, D. L., Coney, P. J., Harms, T. A. & Dillon, J. T. 1988. Interpretive geologic map and supporting radiolarian data from the Angayucham terrane, Coldfoot area, southern Brooks Range, Alaska. *U.S. Geol. Surv. Misc. Field Studies Map* MF-1993, scale 1:63,360.

Julian, F. E. 1989. Structure and stratigraphy of Lower Paleozoic rocks, Doonerak window, central Brooks Range, Alaska. Unpublished Ph.D. thesis, Rice University, Houston, Texas.

Koons, P. O. 1986. Relative geobarometry from high-pressure rocks of quartzofeldspathic composition from the Sezia Zone, Western Alps, Italy. *Contr. Miner. Petrol.* **93**, 322–334.

Lacassin, R. 1987. Kinematics of ductile shearing from outcrop to ductile scale in the Monte Rosa nappe, western Alps. *Tectonics* **6**, 69–88.

Lister, G. S. 1977. Crossed-girdle *c*-axis fabrics in quartzites plastically deformed by plane strain and progressive simple shear. *Tectonophysics* **39**, 51–54.

Lister, G. S. & Hobbs, B. E. 1980. The simulation of fabric development during plastic deformation and its application to quartzite: the effect of deformation path. *J. Struct. Geol.* **2**, 355–370.

Lister, G. S. & Williams, P. F. 1979. Fabric development in shear zones: theoretical controls and observed phenomena. *J. Struct. Geol.* **1**, 283–297.

Lister, G. S. & Williams, P. F. 1983. The partitioning of deformation in flowing rock masses. *Tectonophysics* **92**, 1–33.

Mainprice, D., Bouchez, J.-L., Blumenfeld, P. & Maria Tubiá, J. 1986. Dominant *c*-slip in naturally deforming quartz: implications for dramatic plastic softening at high temperatures. *Geology* **14**, 819–822.

Marlow, P. C. & Etheridge, M. A. 1977. The development of a layered crenulation cleavage in mica schists of the Kanmantoo Group near Macclesfield, South Australia. *Bull. geol. Soc. Am.* **88**, 873–882.

Matthews, A. & Schliestedt, M., 1984. Evolution of the blueschist and greenschist facies rocks of Sifnos, Cyclades, Greece. *Contr. Miner. Petrol.* **88**, 150–163.

Mayfield, C. F., Tailleur, I. L. & Ellersieck, I. 1983. Stratigraphy, structure and palinspastic synthesis of the western Brooks Range, northwestern Alaska. *U.S. Geol. Surv. Open File Report* OFR 83-779, 58 p.

Miller, E. L. 1987. Dismemberment of the Brooks Range orogenic belt during middle Cretaceous extension. *Geol. Soc. Am. Abs. w. Prog.* **19**, 432.

Moore, T. E. & Churkin, M., Jr. 1984. Ordovician and Silurian graptolite discoveries from the Neruokpuk Formation, northeastern and central Brooks Range, Alaska. *Paleozoic Geol. Alaska Nw. Canada Newslett., Alaska geol. Soc.* **1**, 21–23.

Mull, C. G. 1982. Tectonic evolution and structural style of the Brooks Range, Alaska: An illustrated summary. In: *Geologic Studies of the Cordilleran Thrust Belt* (edited by Blake, R. B.). Rocky Mountain Association of Geologists, Denver, 1–45.

Murphy, J. M. & Patton, W. W. 1988. Geologic setting and petrography of the phyllite and metagreywacke thrust panel, north-central Alaska. *U.S. Geol. Surv. Circ.* **1016**, 104–108.

Nelson, B. K., Nelson, S. W. & Till, A. B., 1989. Isotopic evidence of an early Proterozoic crustal source for granites of the Brooks Range, northern Alaska. *Geol. Soc. Am. Abs. w. Prog.* **21**, A105.

Okay, A. I. 1986. High-pressure/low-temperture metamorphic rocks of Turkey. In: *Eclogites and Blueschists* (edited by Evans, B. W. & Brown, E. H.). *Mem. geol. Soc. Am.* **164**, 333–347.

Oldow, J. S., Avé Lallemant, H. G. & Gottschalk, R. R. 1989b. Envelopment thrusting in the central Brooks Range fold and thrust belt, Arctic Alaska. *Geol. Soc. Am. Abs. w. Prog.* **21**, 125.

Oldow, J. S., Bally, A. W., Avé Lallemant, H. G. & Leeman, W. P. 1989a. Phanerozoic evolution of the North American Cordillera: United States and Canada. In: *The Geology of North America—An Overview* (edited by Bally, A. W. & Palmer, A. R.). *Geol. Soc. Am., Geology of North America* A, 139–232.

Oldow, J. S., Gottschalk, R. R. & Avé Lallemant, H. G. 1987b. Low-angle normal faults, southern Brooks Range fold and thrust belt, northern Alaska. *Geol. Soc. Am. Abs. w. Prog.* **19**, 438.

Oldow, J. S., Seidensticker, C. M., Phelps, J. C., Julian, F. E., Gottschalk, R. R., Boler, K. W., Handschy, J. W. & Avé Lallemant, H. G. 1987a. Balanced cross-sections through the central Brooks Range and North Slope, Arctic Alaska. *Spec. Publ. Am. Ass. Petrol. Geol.*

Pallister, J. S. & Budahn, J. R. In press. Pillow basalts of the Brooks Range: oceanic-plateau and island crust accreted to the Brooks Range. *J. geophys. Res.*

Patrick, B. E. 1988. Synmetamorphic evolution of the Seward Peninsula blueschist terrane, Alaska. *J. Struct. Geol.* **10**, 555–566.

Patton, W. W., Jr. 1984. Timing of arc collision and emplacement of oceanic crustal rocks on the margins of the Yukon–Koyukuk basin, western Alaska. *Geol. Soc. Am. Abs. w. Prog.* **16**, 328.

Patton, W. W., Jr. & Tailleur, I. L. 1977. Evidence in the Bering Strait region for differential movement between North America and Eurasia. *Bull. geol. Soc. Am.* **88**, 1298–1304.

Phelps, J. C. 1987. Stratigraphy and structure of the northeastern Doonerak window area, central Brooks Range, northern Alaska. Unpublished Ph.D. thesis, Rice University, Houston, Texas.

Platt, J. P. 1983. Progressive refolding in ductile shear zones. *J. Struct. Geol.* **5**, 619–622.

Platt, J. P. 1986. Dynamics of orogenic wedges and the uplift of high-pressure metamorphic rocks. *Bull. geol. Soc. Am.* **97**, 1037–1053.

Platt, J. P. & Vissers, R. L. M. 1980. Extensional structures in anisotropic rocks. *J. Struct. Geol.* **2**, 397–410.

Pognante, U., Talarico, F., Rastelli, N. & Feratti, N. 1987. High-pressure metamorphism in the nappes of the Valle dell'Orco traverse (Western Alps collisional belt). *J. metamorph. Geol.* **5**, 397–414.

Price, G. P. 1985. Preferred orientations in quartzites. In: *Preferred*

Orientation in Deformed Metals and Rocks: An Introduction to Modern Textural Analysis (edited by Wenk, H.-R.). Academic Press, New York.

Quinquis, H., Audreu, C., Brun, J. P. & Cobbold, P. R. 1978. Intense progressive shear in the Ile de Groix blueschists and compatibility with obduction or subduction. *Nature Lond.* **273**, 43–45.

Ramsay, J. G. 1967. *Folding and Fracturing of Rocks*. McGraw-Hill, New York.

Roeder, D. & Mull, C. G. 1978. Tectonics of the Brooks Range ophiolites, Alaska. *Bull. Am. Ass. Petrol. Geol.* **62**, 1696–1713.

Sanderson, D. J. 1973. The development of fold axes oblique to regional trend. *Tectonophysics* **16**, 55–70.

Schmid, S. M. & Casey, M. 1986. Complete fabric analysis of some commonly observed quartz *c*-axis patterns. In: *Mineral and Rock Deformation: Laboratory Studies* (edited by Hobbs, B. E. & Heard, H. C.). *Am. Geophys. Un. Geophys. Monogr.* **36**, 263–286.

Seidensticker, C. M., Julian, F. E., Oldow, J. S. & Avé Lallemant, H. G. 1987. Kinematic significance of antithetic structures in the central Brooks Range, Alaska. *Geol. Soc. Am. Abs. w. Prog.* **19**, 449.

Spry, A. 1969. *Metamorphic Textures*. Pergamon Press, New York.

Swager, N. 1985. Solution transfer, mechanical rotation and kink-band boundary migration during crenulation cleavage development. *J. Struct. Geol.* **7**, 421–429.

Thurston, S. P. 1985. Structure, petrology, and metamorphic history of the Nome Group blueschist terrane, Salmon Lake area, Seward Peninsula, Alaska. *Bull. geol. Soc. Am.* **96**, 600–617.

Till, A. B. 1988. Evidence for two Mesozoic blueschist belts in the hinterland of the western Brooks Range fold and thrust belt. *Geol. Soc. Am. Abs. w. Prog.* **20**, A112.

Till, A. B., Schmidt, J. M. & Nelson, S. W. 1988. Thrust involvement of metamorphic rocks, southwestern Brooks Range, Alaska. *Geology* **16**, 930–933.

Tobisch, O. T. & Paterson, S. R. 1988. Analysis and interpretation of composite foliations in areas of progressive deformation. *J. Struct. Geol.* **10**, 745–754.

Tullis, J. 1977. Preferred orientation of quartz produced by slip during plane strain. *Tectonophysics* **39**, 87–102.

Tullis, J., Christie, J. M. & Griggs, D. T. 1973. Microstructures and preferred orientations of experimentally deformed quartzites. *Bull. geol. Soc. Am.* **84**, 297–314.

Turner, D. L., Forbes, R. B. & Dillon, J. T. 1979. K-Ar geochronology of the southwestern Brooks Range, Alaska. *Can. J. Earth Sci.* **16**, 1789–1804.

Turner, F. J. & Weiss, L. E. 1963. *Structural Analysis of Metamorphic Tectonites*. McGraw-Hill, New York.

White, S. H. 1973. The dislocation structures responsible for the optical effects in some naturally deformed quartzites. *J. Mater. Sci.* **9**, 69–86.

White, S. H. 1976. The effects of strain on the microstructures, fabrics and deformation mechanisms in quartz. *Phil. Trans. R. Soc. Lond.* **A283**, 69–86.

Zwart, H. J. 1962. On the determination of polymetamorphic mineral associations and its application to the Bosost area (coastal Pyrenees). *Geol. Rdsch.* **52**, 38–65.